Templated Synthesis of Cuprous Chloride Networks: Synthesis and Characterization of $[Hpy]Cu_3Cl_6$ and $\{[H_3NMe]_6Cl\}[H_3NMe]_2Cu_9Cl_{16}$

James D. Martin,* Jincai Yang, and Andrew M. Dattelbaum

Department of Chemistry, North Carolina State University, Raleigh, North Carolina 27695-8204

Received August 17, 2000. Revised Manuscript Received November 1, 2000

Solvothermal reactions with a 1:1 ratio of cuprous chloride and alkylamonium salts as templating agents in acetonitrile or ethanol yield two new polyanionic chains. The trimeric chain $[Cu_3Cl_6]^{3-}$, **1**, templated by pyridinium cations, crystallizes in the monoclinic space group $P2_1/m$ with $a = 9.1274(8)$ Å, $b = 13.2831(5)$ Å, $c = 10.0923(7)$ Å, $\beta = 112.562(5)°$, and $Z = 2$. $[Cu_9Cl_{16}]_n^{7-}$ **2**, is templated by the complex cation $\{[H_3NMe]_6Cl\}^{5+}$ and two independent $[H_3NMe]^+$ cations. The polyanionic chain of **2** is constructed from the condensation of tetrameric cuprous chloride building blocks and crystallizes in the triclinic space group $P\bar{1}$ with $a = 10.091(2)$ Å, $b = 10.173(2)$ Å, $c = 23.723(3)$ Å, $\alpha = 80.12(1)°$, $\beta = 80.99(1)°$, $\gamma = 70.68(2)°$, and $Z = 2$. The targeted stoichiometry of $[A][CuCl_2]$, with A = pyridinium or methylammonium as templates, results in the formation of condensed oligomeric building blocks that are analogous to those observed for a variety of open-framework group 13 chalcogenides. The relationship between the charge density of the templating species and of the inorganic building blocks is discussed with respect to general principles for the construction of open frameworks.

Introduction

The coordination chemistry of Cu^I in metal halides and chalcogenides is quite varied, commonly exhibiting both three and four coordination.[1] The low energetic cost for coordinative flexibility at copper contributes to the common observation of ionic conduction[2] and reactivity at the Cu^I site in numerous organic[3] and biochemical[4] reactions. The coordinative flexibility and reactivity of Cu^I was attractive to us as a target building block for the construction of open-framework metal halide materials. Previously, we demonstrated the possible structural analogy between $CuCl_4^{3-}$ and PS_4^{3-} for the preparation of mixed metal halide species in the presence of Al^{III} [5] or Zr^{IV}.[6] On the basis of a possible analogy to aluminate zeolite-type frameworks, $[Al_nO_{2n}]^{n-}$, we initiated an investigation of templated syntheses of copper chlorides in an effort to prepare $[Cu_nCl_{2n}]^{n-}$ open-framework materials.

The design of open-framework materials remains a significant challenge both in terms of the syntheses as well as in the understanding of the principles of structure and bonding that direct the formation of extended structures. In a system such as the templated cuprous chlorides described here, the template:CuCl composition ratio, {ACl:CuCl}, and the respective charge density of the template are critical parameters for the control of structural design. The general influence of these on network formation is schematically represented below. By disrupting the zinc blende-type, condensed three-dimensional network structure of CuCl (*low inorganic charge density*) with templating species, it is rather intuitive to suggest that the greatest portion of the inorganic network will be retained for systems with low {ACl:CuCl} ratios, particularly, for small, high-charge-density templates. As the charge density of the inorganic component is increased or that of the template is decreased, the network structure will be broken down. Variation of the {ACl:CuCl} composition ratios readily controls the inorganic charge density. For example, CuCl {0:1} and the isolated molecular anion, $[CuCl_4]^{3-}$ {3:1}, represent the charge density limits for the cuprous chloride system. Variation of the alkyl substituents of alkylammonium cationic templates provides a considerable range of charge density that can be accessed to probe the influence of templates on network formation.

		Inorganic Charge Density	
		High	Low
Template Charge Density	High	low-dimensional networks and chains	3-D networks
	Low	chains or molecular anions	low-dimensional networks and chains

(1) Burdett, J. K.; Eisenstein, O. *Inorg. Chem.* **1992**, *31*, 1758.
(2) Huggins, R. A. In *Diffusion in Solids*; Nowick, A. S., Burton, J. J., Eds.; Academic Press: New York, 1975; p 445.
(3) Taylor, R. J. K., Ed. *Organocopper Reagents: A Practical Approach*; Oxford University Press: Oxford, 1994.
(4) Karlin, K. D., Tyeklár T., Eds. *Bioinorganic Chemistry of Copper*; Chapman & Hall: New York, 1993.
(5) (a) Martin, J. D.; Leafblad, B. R.; Sullivan, R. M.; Boyle, P. D. *Inorg. Chem.* **1998**, *37*, 1341. (b) Sullivan, R. M.; Martin, J. D. *J. Am. Chem. Soc.* **1999**, *122*, 10092.
(6) (a) Dattelbaum, A. M.; Martin, J. D. *Inorg. Chem.* **1999**, *38*, 2369. (b) Dattelbaum, A. M.; Martin, J. D. *Inorg. Chem.* **1999**, *38*, 6200.

10.1021/cm0006648 CCC: $20.00
Published on Web 01/05/2001

To create network structures, we have explored syntheses of the more inorganic-rich compositions $[Cu_nCl_{2n}]^{n-}$, $n \geq 1$, (low inorganic charge density) with relatively small monovalent cations (reasonably high template charge density). From this work two new network-chain structures have been discovered and crystallographically characterized. The $[Cu_3Cl_6]^{3-}$ structure consists of linked trimer units organized through hydrogen bonding to the pyridinium cationic templates. The $[Cu_9Cl_{16}]^{7-}$ network chain of linked super-tetrahedral complex anions is organized around the unique, composite cation $\{[H_3NMe]_6Cl\}^{5+}$.

Experimental Section

General Procedures. All reactions were performed under an inert atmosphere of dry N_2 in a glovebox or using Schlenk line techniques. The CuCl was prepared from Cu metal and $CuCl_2$ (Aldrich) according to literature methods and further purified by sublimation.[7] Acetonitrile (99.9%, Fisher) was distilled from Na/benzophenone and then stored under nitrogen and over molecular sieves. Ethanol (AAPER Alcohol) was distilled and then stored under nitrogen and over molecular sieves. Pyridine hydrochloride (HpyCl) and methylammine hydrochloride (H_3NMeCl) (98%, Aldrich) were dried by sublimation under dynamic vacuum at 80−90 °C. *Note of Caution: for all solvothermal reactions the sealed reaction vessels build up significant pressure upon heating, which can lead to vessel rupture. Appropriate shielding should be utilized such as placing the reaction vessels in a capped iron pipe during heating. Furthermore, solvothermal reaction vessels should never be filled to greater than 80 vol % to avoid hydraulic-type pressure.*[8] *A filling factor of 25−50% is recommended for the majority of synthetic applications.* All powder X-ray diffraction measurements were obtained using an Enraf-Nonius Guinier camera and were indexed with respect to silicon as a standard.

Synthesis. *Preparation of $[Hpy]_3Cu_3Cl_6$* ***(1)***. A sample of 50 mg of CuCl (0.50 mmol) and 58 mg of HpyCl (0.50 mmol) was placed in a thick walled fused silica tube (10-mm o.d. × 6-mm i.d.). On a Schlenk line, 2.0 mL of acetonitrile were added to the reaction vessel. The reaction mixture was frozen with liquid N_2 and sealed using a torch such that the fused silica vessel was filled to 25% volume. The reaction mixture was heated to 100 °C overnight and then cooled to room temperature by turning off the furnace. All material remained in solution after cooling to room temperature. The reaction vessel was then placed in a −15 °C freezer. After 2−3 days a >92% yield of pale yellow crystals (mp 131 °C) of **1** were isolated. A crystal suitable for a single-crystal X-ray diffraction study was obtained and the homogeneity of the bulk sample was confirmed by powder X-ray diffraction.

Preparation of $\{[H_3NMe]_6Cl\}[H_3NMe]_2Cu_9Cl_{16}$ ***(2)***. A sample of 60 mg of CuCl (0.61 mmol) and 41 mg of H_3NMeCl (0.61 mmol) was placed in a thick walled fused silica tube (10-mm o.d. × 6-mm i.d.). On a Schlenk line, 1.5 mL of ethanol was added to the reaction vessel. The reaction mixture was frozen with liquid N_2 and sealed using a torch such that the fused silica vessel was filled to 25% volume. The reaction mixture was heated to 100 °C for 4 days. A small amount of undissolved CuCl remained in the reaction vessel at these conditions. Working behind appropriate shielding, the reaction vessel was inverted in the oven to decant the solution away from the unreacted CuCl. The sample was then slow cooled to room temperature by turning off the oven. Colorless needle-shaped crystals of **2** (mp 86 °C) were isolated in a 70% yield. A crystal suitable for a single-crystal X-ray diffraction study was obtained and the homogeneity of the bulk sample was confirmed by powder X-ray diffraction.

Single-Crystal X-ray Diffraction. *$[Hpy]_3Cu_3Cl_6$* ***(1)***. A pale yellow crystal of **1** with dimensions 0.3 × 0.3 × 0.2 mm was mounted in a Pyrex capillary under dry N_2 using silicon grease. Single-crystal X-ray data were collected on an Enraf-Nonius CAD4 diffractometer at 293 K using Mo Kα radiation (λ = 0.71073 Å). Final cell constants of a = 9.1274(8), b = 13.2831(7), c = 10.0923(7), and β = 112.562(5)° were determined by a symmetry constrained fit of 24 well-centered reflections (28° < 2θ < 38°) and their Friedel pairs. A quadrant of data, $\pm h$, k, l, with 3392 unique reflections was collected by the $\theta/2\theta$ scan mode out to θ < 30°. Data were scaled to the intensity check reflections using a five-point smoothing curve fitting routine. An empirical absorption correction was applied using psi scan data.

Systematic absences were found to be consistent with the monoclinic space group $P2_1/m$, which was confirmed in the subsequent refinement. The structure was refined using the NRCVAX suite of programs.[9] All non-hydrogen atoms were located by direct methods using the SIR92 program[10] and refined anisotropically. Hydrogen atoms bound to the pyridinium cations were added in calculated positions and assigned fixed temperature factors. A full-matrix least-squares calculation using the 1368 unique reflections ($I > 2.5\sigma(I)$) with 133 parameters gave a final refinement with R factors of R = 0.048 and R_w = 0.054. The final difference map was flat with the largest peak of 0.480 $e^-/Å^3$.

$\{[H_3NMe]_6Cl\}[H_3NMe]_2Cu_9Cl_{16}$. A colorless crystal of **2** with dimensions 0.18 × 0.10 × 0.06 mm was mounted in a Pyrex capillary under dry N_2 using silicon grease. Single-crystal X-ray data were collected on an Enraf-Nonius CAD4 diffractometer at 293 K using Mo Kα radiation (λ = 0.71073 Å). Final cell constants for the triclinic cell, a = 10.091(2), b = 10.173(2), c = 23.723(3), α = 80.11(1)°, β = 99.284(7)°, and γ = 70.67(2)°, were determined by a symmetry constrained fit of 24 well-centered reflections (18° < 2θ < 26°) and their Friedel pairs. A hemisphere of data, $\pm h$, k, $\pm l$, with 7804 unique reflections was collected by the $\theta/2\theta$ scan mode out to θ < 25°. The three standard reflections, measured every 4800 s, did not vary more than 2% throughout the data collection. An empirical absorption correction was applied using psi scan data.

Data were consistent with the triclinic space group $P\bar{1}$, which was confirmed in the subsequent refinement. The structure was refined using the NRCVAX suite of programs.[9] All non-hydrogen atoms were located by direct methods using the SIR92 program[10] and the Cu, Cl, and N atoms were refined anisotropically. Carbon and nitrogen atoms were differentiated based on the short contacts to chlorides. Atoms with contacts of less than 3.5 Å to chloride were designated as N. Carbon atoms could only be refined isotropically. Hydrogen atoms of the methylammonium cations could not be located and were not included in the final refinement. A full-matrix least-squares calculation using the 3442 unique reflections ($I > 1.0\sigma(I)$) with 339 parameters gave a final refinement with R factors of R = 0.077 and R_w = 0.069. The final difference map was flat with the largest peak of 0.960 $e^-/Å^3$.

Results

A summary of the crystallographic data for $[Hpy]_3Cu_3Cl_6$, **1**, and $\{[H_3NMe]_6Cl\}[H_3NMe]_2Cu_9Cl_{16}$, **2**, is given in Table 1.

$[Hpy]_3Cu_3Cl_6$, 1. A ball-and-stick drawing of the basic trimer building unit of **1** is shown in Figure 1, indicating the atom numbering scheme. Positional parameters are given in Table 2, and selected bond distances, bond angles, and hydrogen-bond contacts are given in Tables 3 and 4, respectively. These trimeric units lie across a mirror plane of symmetry and are linked along the 2_1 axis through sharing Cl(1) along b

(7) Kauffman, G. B.; Fang, L. Y. *Inorg. Synth.* **1983**, *22*, 101.
(8) Rabenau, A. *Angew. Chem., Int. Ed. Engl.* **1985**, *24*, 1026.
(9) Gabe, E. J.; Le Page, Y.; Charland, J.-P.; Lee, F. L.; White, P. S. *J. Appl. Crystallogr.* **1989**, *22*, 384.
(10) Altomare, A.; Burla, M. C.; Camulli, G.; Cascarano, G.; Giacovazzo, C.; Guagliardi, A.; Polidori, G. *J. Appl. Crystallogr.* **1994**, *27*, 435.

Table 1. Crystallographic Data for $[Hpy]_3Cu_3Cl_6$ (1) and $\{[H_3NMe]_6Cl\}[H_3NMe]_2Cu_9Cl_{16}$ (2)

formula	$[Hpy]_3Cu_3Cl_6$	$\{[H_3NMe]_6Cl\}[H_3NMe]_2Cu_9Cl_{16}$
fw (g/mol)	643.68	1430.74
temp (°C)	25	25
space group (No.)	$P2_1/m$ (11)	$P\bar{1}$ (2)
a (Å)	9.1274(8)	10.091(2)
b (Å)	13.2831(5)	10.173(2)
c (Å)	10.0923(7)	23.723(3)
α (deg)		80.12(1)
β (deg)	112.562(5)	80.99(1)
γ (deg)		70.68(2)
V (Å^3)	1129.9(1)	2251.0(7)
Z	2	2
ρ_{calcd} (mg cm^{-3})	1.892	2.040
λ(Mo Kα) (Å)	0.71073	0.71073
μ (cm^{-1})	35.3	52.2
R^a	0.048	0.077
$R_w{}^b$	0.054	0.069

^{a} $R_f = \sum(F_o - F_c)/F_o$. ^{b} $R_w = [\sum(w(F_o - F_c)^2)/wF_o^2)]^{1/2}$.

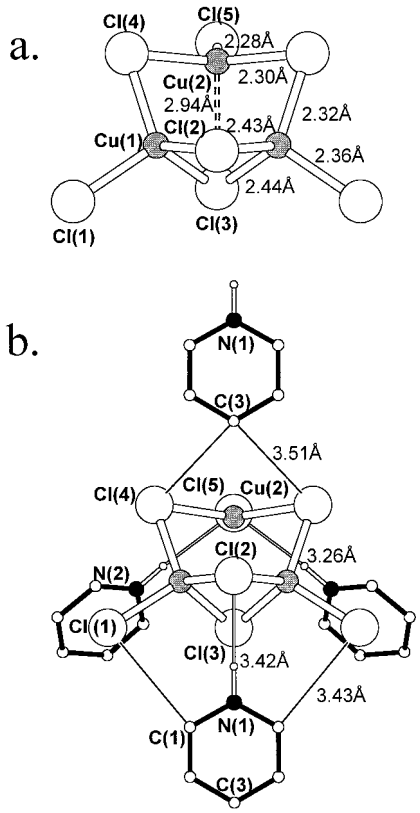

Figure 1. Ball and stick drawings of the Cu_3Cl_7 trimer in **1**, which emphasize (a) the structural distortions of the Cu−Cl distances and (b) the hydrogen bond contacts to the pyridinium cations.

as shown by the ORTEP drawing in Figure 2a. It is possible to describe the structure of the trimeric complex in **1** as a distorted version of the $[In_3Te_7]^{5-}$ anion[11] in which the three metal cations are each bridged by a μ^2−Cl and each has one terminal ligand. The trimer is then capped by a μ^3−Cl. In the polymeric anion $[Cu_3Cl_6]^{3-}$ two of the "terminal" chlorides bridge neighboring trimers to form the chain. There is a major distortion to this trimeric unit; however, resulting in the elongation of the Cu(2)−Cl(3) distance to 2.942(3) Å, while the two Cu(1)−Cl(3) distances are 2.440(2) Å. This distortion leaves Cu(2) effectively with a coordination number

(11) Park, C.-W.; Salm, R. J.; Ibers, J. A. *Angew. Chem., Int. Ed. Engl.* **1995**, *34*, 1879.

Table 2. Atomic Coordinates and Isotropic Displacement Parameters for $[Hpy]_3Cu_3Cl_6$ (1)

	x	y	z	B_{iso}
Cu(1)	0.4235(1)	0.85599(7)	0.8519(1)	5.44(6)
Cu(2)	0.2084(2)	3/4	0.6088(2)	5.28(7)
Cl(1)	1/2	0	0	5.6(2)
Cl(2)	0.6582(3)	3/4	0.9184(3)	4.9(1)
Cl(3)	0.2376(3)	3/4	0.9094(2)	3.6(1)
Cl(4)	0.3157(2)	0.9072(1)	0.6144(2)	3.98(8)
Cl(5)	0.9385(3)	3/4	0.5047(3)	5.0(1)
N(1)	0.574(1)	3/4	0.2206(9)	6.3(6)
N(2)	0.049(1)	0.0567(6)	0.2917(8)	7.5(5)
C(1)	0.5618(8)	0.8377(6)	0.2814(8)	4.6(4)
C(2)	0.5374(8)	0.8377(5)	0.4039(9)	4.8(4)
C(3)	0.524(1)	3/4	0.468(1)	4.4(5)
C(4)	0.971(1)	0.976(1)	0.274(1)	8.1(7)
C(5)	0.002(2)	0.9005(8)	0.202(1)	9.3(8)
C(6)	0.120(2)	0.9111(9)	0.152(1)	8.2(7)
C(7)	0.194(1)	0.999(1)	0.169(1)	8.9(8)
C(8)	0.159(2)	0.070(1)	0.239(1)	9.5(8)

Table 3. Selected Bond Distances (Å) and Bond Angles (deg) for $[Hpy]_3Cu_3Cl_6$ (1)

Cu(1)−Cu(1)	2.816(2)	Cl(2)−Cu(2)−Cl(3)	62.97(6)
Cu(1)−Cu(2)	2.857(2)	Cl(2)−Cu(2)−Cl(4) ×2	71.83(5)
		Cl(2)−Cu(2)−Cl(5)	160.4(1)
Cu(1)−Cl(1)	2.362(1)		
Cu(1)−Cl(2)	2.433(2)	Cl(3)−Cu(2)−Cl(4) ×2	96.05(6)
Cu(1)−Cl(3)	2.440(2)	Cl(3)−Cu(2)−Cl(5)	97.5(1)
Cu(1)−Cl(4)	2.316(2)		
		Cl(4)−Cu(2)−Cl(4)	130.68(8)
Cu(2)−Cl(3)	2.942(3)	Cl(4)−Cu(2)−Cl(5) ×2	112.74(5)
Cu(2)−Cl(4) ×2	2.298(2)		
Cu(2)−Cl(5)	2.277(3)	Cl(1)−Cu(1)−Cl(2)	106.20(6)
		Cl(1)−Cu(1)−Cl(3)	112.35(6)
		Cl(1)−Cu(1)−Cl(4)	108.79(5)
		Cl(1)−Cu(1)−Cl(4)	175.92(4)
		Cl(2)−Cu(1)−Cl(3)	102.68(7)
		Cl(2)−Cu(1)−Cl(4)	115.79(9)
		Cl(2)−Cu(1)−Cl(4)	70.09(6)
		Cl(3)−Cu(1)−Cl(4)	110.94(8)
		Cl(3)−Cu(1)−Cl(4)	67.52(5)
		Cl(4)−Cu(1)−Cl(4)	74.73(5)

of three. Thus, this distorted trimer alternatively can be described as an edge-shared tetrahedral dimer, Cu_2Cl_6, in which two of the terminal chlorides have been tied back by a CuCl bridge and the other two terminal chlorides form the chain linkages. The edge-shared dimer is only slightly distorted with the chloride bridges of the dimer being about 0.1 Å longer than the other Cu−Cl distances. While the Cl(1), Cl(1′), Cl(4), Cl(4′), Cu(1), and Cu(1′) atoms are all coplaner, the bridging Cu(2)−Cl(5) unit is bent 79.6° away from this plane. Cl(5) is the only terminal chloride in this structure and is bound 2.277(3) Å from Cu(2). The trigonal Cu(2) exhibits bond angles of Cl(4)−Cu(2)−Cl(5) = 112.74(5)° (×2) and Cl(4)−Cu(2)−Cl(4) = 130.68(8)°.

Hydrogen bonding to the pyridinium cations plays a significant role in the distortion of this cuprous chloride polyanion as well as in the organization of the polymeric chains into the crystalline network. As seen in Figure 1b, strong hydrogen bonding is observed between the chlorides and the edges of the pyridinium rings with short CH···Cl and NH···Cl contacts. The CH···Cl interactions arise from the δ^+ charge on the edge of the aromatic ring. The pyridinium cation containing N(1) is hydrogen bonded with short N(1)−Cl(2) = 3.420(9) Å and two C(1)−Cl(1) = 3.435(7) Å contacts to one side of the cuprous chloride trimer and with two C(3)−Cl(4) = 3.514(7) Å contacts to the other side of a neighboring trimer, thus linking polymeric chains. An additional

Table 4. Hydrogen Bonding in $[Hpy]_3Cu_3Cl_6$(1) (N−Cl and C−Cl Distances Are Given in Å)

	N(1)	N(2)	C(1)	C(2)	C(3)	C(4)	C(8)
Cl(1)			3.435(7) ×2				
Cl(2)	3.420(9)						3.61(1)
Cl(3)	3.447(9)						
Cl(4)			3.597(8)	3.573(7)	3.514(7) ×2	3.58(1)	
Cl(5)	3.461(9)	3.262(7) ×2	3.509(7)	3.597(7)			

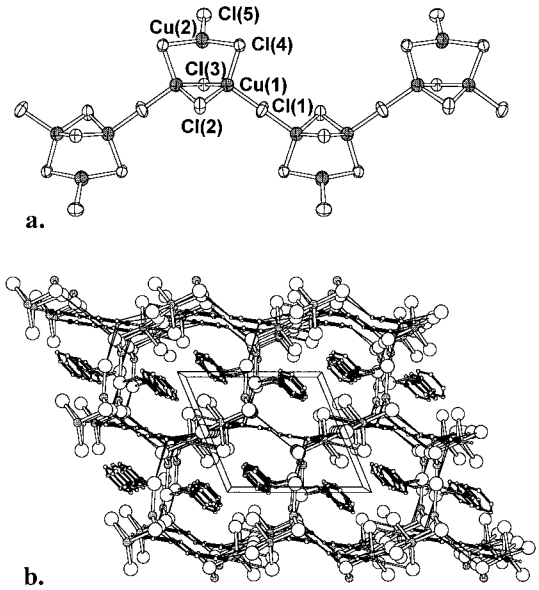

Figure 2. (a) ORTEP drawing of the $[Cu_3Cl_6]^{3-}{}_n$ chain of trimers and (b) crystal packing view down the crystallographic *b* axis, indicating the hydrogen-bonded network formed with the pyridinium cation associated with N(1) and the N(2) pyridinium cations stacked in the channels.

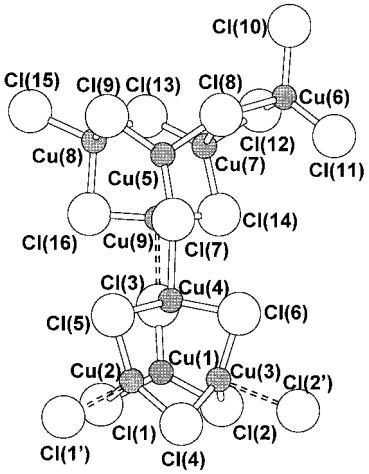

Figure 3. Ball and stick drawing of the Cu_9Cl_{18} dimer-of-tetramers, which is the building block of the polyanionic cuprous chloride chain in **2**.

contact of 3.509(7) Å is observed between C(1) and Cl(5), which is orthogonal to the ring plane and may be related to a small amount of charge transfer, resulting in the pale yellow color of the crystalline material. As is readily apparent from the crystal packing view in Figure 2b, the hydrogen bonding around the entire edge of this pyridinium ring to chlorides of adjacent chains effectively link these polyanionic chains into an open framework. In these channels two pyridinium cations form two strong hydrogen bonds to the only terminally coordinated chloride ligand, N(2)H···Cl(5) = 3.262(7) Å. The shortest contact between the CH edges of the N(2)−pyridinium ring to the nearest neighbor chlorides is C(4)−Cl(4) = 3.58(1) Å. Ring−ring interactions, traditionally referred to as π-stacking, likely contribute toward the stabilization of this lattice; however, none are particularly short. The shortest inter-ring contacts are 3.6 Å, corresponding to stacks of the N(2)−pyridinium cations within the channel structure. It is interesting to note that the shortest Cu−Cl bond is to Cl(5) = 2.227(3) Å, which also receives the strongest hydrogen-bonding interactions, whereas the longest CuCl bonds are to Cl(2) = 2.433(2) Å and Cl(3) = 2.440(2) Å, the latter of which effectively sees no hydrogen-bonded contacts.

{$[H_3NMe]_6Cl$}$[H_3NMe]_2Cu_9Cl_{16}$, 2. The structure of **2** is built from the oligomerization of dimers of copper chloride tetramers, shown as a ball-and-stick representation in Figure 3. Positional parameters are given in Table 5 and selected bond distances, bond angles, and hydrogen-bond contacts are given in Tables 6−8, respectively. The tetramers, with the Cu_4Cl_6 core, exhibit an approximate tetrahedral, adamantine-type geometry. These dimers-of-tetramers are linked with inversion symmetry via an inner/outer halide bridging $(Cl(1)^i/(1')^a$ and $Cl(2)^i/(2')^a)$ to form the chains running along the (1,−1,0) direction shown in Figure 4a. One of the tetrameric units serves as the polymer backbone; the other is "decoration" to the polymer and is also flanked by the additional Cu(6) tetrahedron. These chains have a large width:height aspect ratio (≈8), and thus they are stacked like boards in the crystalline lattice as shown in Figure 4b. When viewed down the *a* crystallographic axis (Figure 4c), a channel-like structure is apparent surrounding some of the templating cations and the isolated chloride, Cl(17).

The $M_4X^i{}_6X^a{}_4$-type tetrameric unit, constructed from four corner-sharing tetrahedra forming a tetrahedron-of-tetrahedra, is a common structural feature observed in other copper−chloride networks[12−15] as well as in numerous metal chalcogenides.[16−19] In **2**, however, significantly large distortions to the tetrameric units are observed. With the exception of the nearly ideal Cu(8) tetrahedron, the outer halides at each tetramer vertex are significantly elongated to between 2.5 and 2.8 Å, while Cu(1) and Cu(5) exhibit no outer halide coordination. Examination of the bond angles in Table 7 shows further indication of this distortion with a near trigonal

(12) Sishen, X.; Geller, S. *J. Solid State Chem.* **1986**, *63*, 326.
(13) Geller, S.; Sishen, X. *J. Solid State Chem.* **1986**, *63*, 316.
(14) Gaines, J. M.; Geller, S. *J. Electrochem. Soc.* **1986**, *133*, 1501.
(15) Mykhalichko, B. M.; Mys'kiv, M. G.; Zavalii, P. Y.; Mazus, M. D.; Osechkin, S. I. *Koord. Khim.* **1991**, *17*, 827.
(16) MacLachlan, M. J.; Petrov, S.; Bedard, R. L.; Manners, I.; Ozin, G. A. *Angew. Chem., Int. Ed.* **1998**, *37*, 2076.
(17) Dance, I. G.; Garbutt, R. G.; Craig, D. C. Scudder, M. L. *Inorg. Chem.* **1987**, *26*, 4057.
(18) Tan, K.; Darovsky, A.; Parise, J. B. *J. Am. Chem. Soc.* **1995**, *117*, 7039.
(19) Li, H.; Laine, A.; O'Keeffe, M.; Yaghi, O. M. *Science* **1999**, *283*, 1148.

Table 5. Atomic Coordinates and Isotropic Displacement Parameters for {[$H_3NMe]_6Cl$}[$H_3NMe]_2Cu_9Cl_{16}$ (2)

	x	*y*	*z*	B_{iso}
Cu(1)	0.1222(3)	0.6220(3)	0.5377(1)	3.8(2)
Cu(2)	0.3899(3)	0.6443(3)	0.5459(1)	4.9(2)
Cu(3)	0.1442(3)	0.8889(3)	0.5457(1)	5.1(2)
Cu(4)	0.1713(3)	0.6681(3)	0.6506(1)	5.0(2)
Cu(5)	0.9727(3)	0.4714(3)	0.7445(1)	5.2(2)
Cu(6)	0.0386(3)	0.5123(3)	0.8462(1)	4.0(2)
Cu(7)	0.0525(3)	0.2142(3)	0.8486(1)	4.9(2)
Cu(8)	0.7488(3)	0.5302(3)	0.8390(1)	4.7(2)
Cu(9)	0.5778(3)	0.7700(3)	0.9138(1)	4.7(2)
Cl(1)	0.3258(5)	0.4840(5)	0.4954(2)	3.5(3)
Cl(2)	0.9866(5)	0.8240(5)	0.4918(2)	3.4(3)
Cl(3)	0.0336(5)	0.5374(5)	0.6241(2)	3.0(3)
Cl(4)	0.3554(6)	0.8576(5)	0.4928(2)	3.9(3)
Cl(5)	0.4096(5)	0.5526(6)	0.6384(2)	3.7(3)
Cl(6)	0.0509(6)	0.9055(5)	0.6374(2)	3.7(3)
Cl(7)	0.1071(6)	0.2485(6)	0.7462(2)	4.8(4)
Cl(8)	0.1150(6)	0.6213(6)	0.7627(2)	4.0(3)
Cl(9)	0.7492(6)	0.6182(6)	0.7432(2)	4.8(3)
Cl(10)	0.1643(6)	0.3248(5)	0.9001(2)	4.0(3)
Cl(11)	0.8422(5)	0.6468(5)	0.8988(2)	3.2(3)
Cl(12)	0.8040(5)	0.2946(5)	0.8714(2)	3.3(3)
Cl(13)	0.1399(6)	0.9750(6)	0.8826(2)	4.6(3)
Cl(14)	0.4904(5)	0.6178(5)	0.8777(2)	3.1(3)
Cl(15)	0.5251(5)	0.7402(5)	0.0131(2)	3.0(3)
Cl(16)	0.5540(5)	0.9886(5)	0.8688(2)	3.6(3)
Cl(17)	0.4160(6)	0.9350(5)	0.3126(2)	3.1(3)
N(1)	0.610(2)	0.102(2)	0.2162(7)	5(1)
N(2)	0.712(2)	0.418(2)	0.9975(6)	3.2(9)
N(3)	0.681(2)	0.7315(16)	0.3757(7)	3.4(9)
N(4)	0.232(2)	0.175(2)	0.3883(7)	4(1)
N(5)	0.479(2)	0.323(2)	0.8475(6)	3.3(8)
N(6)	0.296(2)	0.040(2)	0.9823(6)	3.6(9)
N(7)	0.247(2)	0.739(2)	0.3894(7)	5(1)
N(8)	0.856(3)	0.896(2)	0.793(1)	16(2)
C(1)	0.658(2)	0.158(2)	0.261(1)	5.5(6)
C(2)	0.847(2)	0.369(2)	10.0228(9)	5.0(5)
C(3)	0.726(3)	0.828(3)	0.405(1)	6.0(6)
C(4)	0.339(2)	0.224(2)	0.4100(9)	4.9(5)
C(5)	0.484(2)	0.355(2)	0.7813(9)	5.0(5)
C(6)	0.179(2)	0.044(2)	10.0272(9)	4.8(5)
C(7)	0.188(3)	0.680(3)	0.350(1)	6.3(6)
C(8)	0.891(3)	0.003(3)	0.780(10)	5.5(6)

planar coordination for Cu(1) and Cu(5) and a distortion toward trigonal planar geometry for all copper cations except Cu(8). The distortions of the individual tetrahedra making up the dimer-of-tetramers coincide with their respective structural function. The pairs of Cu(2)/Cu(2′), Cu(3)/Cu(3′), and Cu(4)/Cu(9) tetrahedra link neighboring tetramers and the Cu(7)/Cu(6) pair of tetrahedra link the nonbackbone tetramer to the flanking Cu(6) tetrahedron. The Cu(1) and Cu(5), which both exhibit only a coordination number of three, are the caps of the respective tetramers, leaving only Cu(8), which participates least in the oligomerization, to adopt a nearly ideal tetrahedral geometry. The extensive chloride bridging results in relatively short Cu−Cu contacts (2.7−3.0 Å), the shortest being Cu(5)−Cu(9) = 2.733(4) Å in which Cu(5) is uncharacteristically pulled in toward the center of the tetrameric cage.

Hydrogen bonding to the methylammonium cations is instrumental in templating the decoration of the polymers in **2** as well as being vital to binding the polymer chains together into the crystalline lattice. The hydrogen bonding likely also contributes to the distortions within the tetrameric units. With three ammonium protons per methylammonium cation, the hydrogen bonding throughout this network is quite complex as summarized in Table 8. There are basically

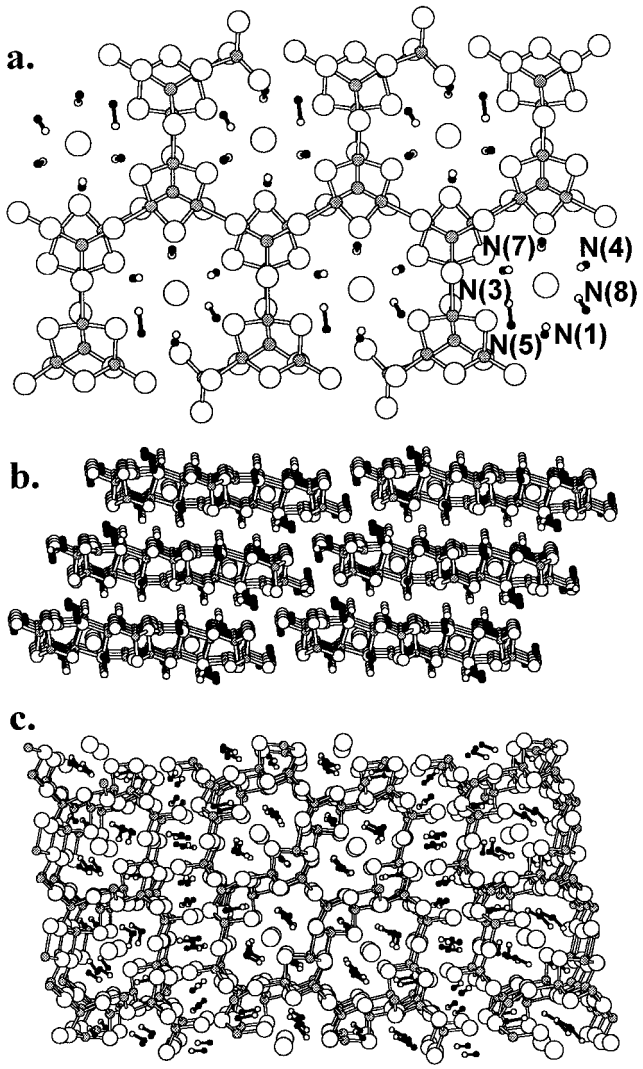

Figure 4. (a) Drawing of the $[Cu_9Cl_{16}]^{7-}{}_n$ chain of the dimers-of-tetramers, emphasizing the organization of the {[H_3-$NMe]_6Cl$}$^{5+}$ complex cation and crystal packing drawings demonstrating (b) the board-like stacking of the polyanionic chains parallel to the 112 crystallographic planes and (c) channel-like features created by the complex cations as viewed down the *a* crystallographic axis.

two types of methylamonium cations in **2**. The cations associated with N(2) and N(6) lie in the layer gap between polymeric chains, best seen in Figure 4b. The hydrogen bonding from these cations link the edges of the polyanionic chains, thus forming a three-dimensional network. The remaining six methylammonium cations, associated with N(1), N(3), N(4), N(5), N(7), and N(8), are organized in an approximately octahedral configuration around an isolated chloride anion to yield a {[$H_3NMe]_6Cl$}$^{5+}$ composite cation. Only four of these six methylammonium cations form short hydrogen-bonded contacts to the isolated chloride, however. N(8), which exhibits the largest thermal ellipsoids in the crystal structure, is oriented such that the N(8)−Cl(17) = 3.78(2) Å is approximately equivalent to the C(8)−Cl(17) = 3.89(2) Å distance. And N(5) is 4.76(2) Å from Cl(17) with a closer contact by Cl(17)−C(5) = 3.78(2) Å. Each of the six methylammonium cations of the composite cation also forms strong hydrogen-bond contacts to the polyanionic chain, resulting in the approximately hexagonal templating of the polymer arms.

Table 6. Selected Bond Distances (Å) for $\{[H_3NMe]_6Cl\}[H_3NMe]_2Cu_9Cl_{16}$ (2)

	Cu(1)	Cu(2)	Cu(3)	Cu(4)	Cu(5)	Cu(6)	Cu(7)	Cu(8)	Cu(9)
Cl(1)	2.263(5)	2.474(6)							
		2.824(5)							
Cl(2)	2.262(5)		2.495(6)						
			2.828(5)						
Cl(3)	2.252(5)			2.423(5)					2.839(5)
Cl(4)		2.263(5)	2.252(5)	2.298(5)					
Cl(5)		2.245(5)							
Cl(6)			2.240(5)	2.307(5)					
Cl(7)				2.626(5)	2.254(5)				2.540(5)
Cl(8)					2.318(5)	2.543(5)	2.461(5)		
Cl(9)					2.223(5)			2.404(5)	
Cl(10)						2.324(5)			
Cl(11)						2.248(5)			
Cl(12)						2.343(5)	2.532(5)		
Cl(13)							2.291(5)	2.372(5)	
Cl(14)							2.296(5)		2.258(6)
Cl(15)								2.341(6)	
Cl(16)								2.394(5)	2.222(6)

Table 7. Selected Bond Angles (deg) for $\{[H_3NMe]_6Cl\}[H_3NMe]_2Cu_9Cl_{16}$ (2)

Cl(1)−Cu(1)−Cl(2)	123.1(2)	Cl(1)−Cu(5)−Cl(2)	116.3(2)
Cl(1)−Cu(1)−Cl(3)	118.2(2)	Cl(1)−Cu(5)−Cl(2)	127.4(2)
Cl(2)−Cu(1)−Cl(3)	118.0(2)	Cl(1)−Cu(5)−Cl(2)	112.3(2)
Cl(1)−Cu(2)−Cl(1′)	87.7(2)	Cl(8)−Cu(6)−Cl(10)	103.6(2)
Cl(1)−Cu(2)−Cl(4)	110.7(2)	Cl(8)−Cu(6)−Cl(11)	103.4(2)
Cl(1)−Cu(2)−Cl(5)	109.2(2)	Cl(8)−Cu(6)−Cl(12)	101.0(2)
Cl(1′)−Cu(2)−Cl(2)	98.9(2)	Cl(10)−Cu(6)−Cl(11)	118.2(2)
Cl(1′)−Cu(2)−Cl(2)	96.4(2)	Cl(10)−Cu(6)−Cl(12)	106.6(2)
Cl(4)−Cu(2)−Cl(5)	137.6(2)	Cl(11)−Cu(6)−Cl(12)	120.9(2)
Cl(2)−Cu(3)−Cl(2′)	90.0(2)	Cl(8)−Cu(7)−Cl(12)	98.2(2)
Cl(2)−Cu(3)−Cl(4)	108.4(2)	Cl(8)−Cu(7)−Cl(13)	110.2(2)
Cl(2)−Cu(3)−Cl(6)	110.0(2)	Cl(8)−Cu(7)−Cl(14)	115.8(2)
Cl(2′)−Cu(3)−Cl(4)	99.4(2)	Cl(12)−Cu(7)−Cl(13)	101.4(2)
Cl(2′)−Cu(3)−Cl(6)	93.9(2)	Cl(12)−Cu(7)−Cl(14)	103.4(2)
Cl(4)−Cu(3)−Cl(2)	139.2(2)	Cl(13)−Cu(7)−Cl(14)	123.1(2)
Cl(3)−Cu(4)−Cl(5)	112.1(2)	Cl(9)−Cu(8)−Cl(13)	110.3(2)
Cl(3)−Cu(4)−Cl(6)	109.8(2)	Cl(9)−Cu(8)−Cl(15)	104.2(2)
Cl(3)−Cu(4)−Cl(7)	97.8(2)	Cl(9)−Cu(8)−Cl(16)	114.0(2)
Cl(5)−Cu(4)−Cl(6)	129.9(2)	Cl(13)−Cu(8)−Cl(15)	109.6(2)
Cl(5)−Cu(4)−Cl(7)	101.7(2)	Cl(13)−Cu(8)−Cl(16)	109.1(2)
Cl(6)−Cu(4)−Cl(7)	98.6(2)	Cl(15)−Cu(8)−Cl(16)	109.5(2)
		Cl(3)−Cu(9)−Cl(7)	89.9(2)
		Cl(3)−Cu(9)−Cl(14)	91.9(2)
		Cl(3)−Cu(9)−Cl(16)	94.2(2)
		Cl(7)−Cu(9)−Cl(14)	104.7(2)
		Cl(7)−Cu(9)−Cl(16)	110.2(2)
		Cl(14)−Cu(9)−Cl(16)	144.5(2)

No hydrogen bonds are observed, however, between the composite cation within one polymer chain to chlorides of a neighboring chain. Instead, an interdigitation of the methyl groups creates a lamellar-type stacking of the respective chains (Figure 4b).

Discussion

Synthesis. The solvothermal syntheses with cuprous chloride in the presence of organic ammonium cations have yielded two new network chain polyanions. Both acetronitrile and ethanol heated in sealed ampules to 100−150 °C are amenable solvents for these reactions. The solvothermal reaction conditions leading to the formation of crystalline species **1** and **2** are primarily important for the solublization of CuCl. In the absence of the solvothermal reaction conditions residual CuCl is always observed. Once the CuCl and template are in solution, the oligomeric species are the favored products because of charge density matching requirements and not because of the forcing solvothermal reaction conditions. After all, crystalline **1** did not precipitate until the solution was cooled to −15 °C.

Table 8. Hydrogen Bonding in $\{[H_3NMe]_6Cl\}[H_3NMe]_2Cu_9Cl_{16}$ (2) (N−Cl Distances Are Given in Å)

	N(1)	N(2)	N(3)	N(4)	N(5)	N(6)	N(7)	N(8)
Cl(1)			3.45(2)				3.27(2)	
Cl(2)				3.32(2)			3.29(2)	
Cl(3)			3.25(2)	3.26(2)				
Cl(4)							3.38(2)	
Cl(5)			3.39(2)					
Cl(6)				3.39(2)				
Cl(7)								3.22(2)
Cl(8)		3.44(1)						3.27(2)
Cl(9)					3.22(1)	3.21(1)		
Cl(10)		3.25(1)			3.25(1)	3.20(1)		
		3.35(1)				3.33(2)		
Cl(11)	3.22(2)				3.19(1)	3.42(2)		3.22(2)
Cl(12)	3.27(2)	3.36(1)			3.25(2)			
Cl(13)		3.32(2)			3.32(2)			
Cl(14)				3.46(2)				
Cl(15)	3.16(2)					3.04(2)		
Cl(16)			3.34(2)					
Cl(17)	3.38(2)		3.19(1)	3.18(2)			3.19(2)	3.78(2)

Network Formation. In an effort to prepare silicate-like, MX_2, corner-shared tetrahedral open-framework structures of cuprous chloride, reactions were loaded with the 1:1 ACl:CuCl (A = Hpy and H_3NMe) stoichiometry. The targeted composition with a stoicheometric charge density intermediate between the highest possible $[CuCl_4]^{3-}$, which yields isolated tetrahedra, and the lowest possible CuCl, which exhibits a zinc-blend-type condensed three-dimensional network, were anticipated to yield more open-framework structures. However, within this composition, the framework charge density can vary by the extent of oligomerization between the isolated $[CuCl_2]^-$ anions observed, with large, low charge density cations,[20,21] and the corner-shared zinc-chloride-type anionic network, which could be expected in the presence of small, high-charge density cations. Although the latter has not yet been observed, it would be the halide analogue of $LiGaS_2$.[22] Given the stoichiometrically imposed charge density (−1 charge per copper center), the more condensed structure would be required for the latter to best charge balance a high

(20) Asplund, M.; Nilsson, M.; Jagner, S. *Acta Chem. Scand.* **1984**, *A38*, 57.
(21) Andersson, S.; Jagner, S. *Acta Chem. Scand.* **1986**, *A40*, 52.
(22) Leal-Gonzalez, J.; Melibary, S. S.; Smith, A. J. *Acta Crystallogr. C* **1990**, *46*, 2017.

charge density cation. With pyridinium as the templating cation, the desired MX_2 stoichiometry was achieved in the $[Cu_3Cl_6]^{3-}$ polyanion, **1**; however, with methylammonium as the template, the slightly metal-rich composition $[Cu_9Cl_{16}]$,$^{7-}$ **2**, was the favored product. For the discussion of the relative condensation of these network chains, it is also instructive to compare them to the edge-shared tetrahedral chain $[CuCl_2]^-$ previously observed with $[NEt_4]^+$, methyl viologen ($[MV]^{2+}$ (1,1′-dimethyl-4,4′-bipyridinium)),[23,24] and ethylenediammonium $[H_2en]^{2+}$,[25] and the network chain of $[Cu_5Cl_9]^{4-}$ templated by Rb^+ cations.[12]

The relative charge density of these templating cations follows the approximate ranking

$$[NEt_4]^+ < [MV]^{2+} < [H_3N(CH_2)_2NH_3]^{2+} < [Hpy]^+ < Rb^+ < [H_3NMe]^+$$

Cations with much lower charge densities, $[N^tBu_4]^+$ and $[NPr_4]^+$, prevent all oligomerization and result in the formation of discrete $[CuCl_2]^-$ linear dimers.[20,21] However, the slightly higher charge density of $[NEt_4]^+$ is sufficient to accommodate the nascence of oligomerization to form the simple edge-shared tetrahedral chain $[CuCl_2]^{n-}$.[23] The relative charge density of the dipositive $[MV]^{2+}$ and $[H_2en]^{2+}$ cationic templates is comparable. But more important for structural direction, the distribution of the positive charges in these dications are also restricted to either end of the rodlike cations, thus favoring the formation of one-dimensional chains. The $[Hpy]^+$, Rb^+, and $[H_3NMe]^+$ cations have a significantly increased charge density, which require modification of the inorganic network to compensate for the charge distribution throughout the crystalline lattice. Because the relative template to cuprous chloride ratio is fixed at ∼1:1 in this series of materials, the only way to increase the charge density of the inorganic network is to increase the extent of $[CuCl_{2n}]^{n-}$ oligomerization. The pyridinium cations have the ability to form π-stacks as well as hydrogen bonds to the cuprous chloride network, and thus, without the methyl groups and the geometric constraints of the $[MV]^{2+}$ cation, exhibit a higher effective charge density as a template. To accommodate this higher charge density requirement, one $[CuCl_2]^-$ unit was effectively added for every two copper units of an edge-shared tetrahedral chain to yield the chain of trimeric $[Cu_3Cl_6]^{3-}$ anions, **2**. In the case of the smaller $[H_3NMe]^+$ and Rb^+ as the templating cations, oligiomerization into polymeric networks built from $Cu_4Cl^i_6Cl^a_{4/2}$ tetramers is required. It is difficult to make a substantive differentiation between the charge density of Rb^+ and $[H_3NMe]^+$. In related work we have shown that Cs^+ and $[H_3NMe]^+$ can be substituted into the same framework void, approximately equivalent in size to one chloride anion in the network structures of $[A]Cu_2Zn_2Cl_7$.[26] Being smaller than Cs^+, the Rb^+ cation, thus, likely has a slightly greater charge density than $[H_3NMe]^+$. Nevertheless, while both the Rb^+-templated $[Cu_5Cl_9]^{4-}$ and the complex-cation-templated $[Cu_9Cl_{16}]^{7-}$ polymeric anions exhibit a polyanionic charge to Cu^+ ratio of 0.8, a slightly increased inorganic network formation is observed for the slightly larger methylammonium templates. This increased network formation in **2** results because six of the methylammonium cations are condensed into the higher charge density $\{[H_3NMe]_6Cl\}^{5+}$ complex cation, by hydrogen bonding to an extraframework chloride anion. This effective "phase separation" of the alkylammonium cations and the cuprous chloride anionic network upon formation of the complex cation in **2** is a process akin to micelle formation. Here, an increased curvature of the polyanionic surface of the low-charge density inorganic network is observed in order to accommodate the higher charge density of the templates. Similar complex cation formation is observed in the more cuprous-chloride-rich three-dimensional network phase, $Rb_4[Cl]_{.39}[Cu_9Cl_{12}]$ (polyanionic charge to Cu^+ ratio of 0.4), in which partially occupied $\{Rb_6Cl\}^{5+}$ complex cations are observed.[14] The concentration of charge by the oligomerization of the cuprous chloride network and the pseuomicelle formation results in a higher lattice energy than would be achieved by a more diffuse distribution of lower charge density building blocks.

A similar process of increasing charge density by oligomerization of the inorganic network to compensate the increased charge density of the template is observed for numerous chalcogenide open framework materials in which analogous trimeric and tetrameric secondary building units are found.[11,16−19,27,28] The formation of condensed structural units in MX_2 chalcogenide materials (M = Ge, Sn, Ga, and In; X = S and Se) is in noted contrast to the open frameworks of corner-shared tetrahedra in the corresponding isoelectronic silicates (SiO_2) and aluminosilicates. In silicates, the high charge density of the oxide anions can effectively compensate the significant charge density of templates without the need for condensation into oligomeric building blocks. By contrast, the larger and more polarizable chalcogenides, like the heavier halides, require the formation of condensed oligomers to achieve the necessary charge density to compensate for the template.

Structural Distortions. The cuprous chloride oligomeric building units $(Cu_3Cl_4)Cl_{3-n}$ and $(Cu_4Cl_6)Cl_{4-n}$ described here are considerably more distorted than related chalcogenide analogues. However, this is primarily due to the difference between the electronic structure of Cu^I and that of Ga, In, Ge, or Sn rather than a difference between anions. The empty 4s and 4p orbitals on copper are low in energy and readily mix with the filled (Cu 3d)-based Cu−Cl σ* orbitals in a second-order Jahn−Teller fashion.[1] Because these empty orbitals are strongly Cu−Cl antibonding, this orbital mixing causes significant structural distortion, frequently from a tetrahedral toward a trigonal planar geometry at copper. Hydrogen bonding between the chloride ligands and the alkylammonium cations also contributes to this second-order Jahn−Teller mixing and thus the structural distortion.[6] A small charge-transfer

(23) Scott, B.; Willett, R.; Porter, L.; Williams, J. *Inorg. Chem.* **1992**, *31*, 2483−2492.
(24) Prout, C. K.; Murry-Rust, P. *J. Chem. Soc.* **1969**, 1520−1525.
(25) Clements, A. C.; Euliss, L. E.; Dattelbaum, A. M.; Martin, J. D. Unpublished results.
(26) Martin, J. D.; Dattelbaum, A. M.; Sullivan, R. M.; Thornton, T. A.; Yang, J.; Peachey, M. T. *Chem. Mater.* **1998**, *10*, 2699.
(27) (a) Jiang, T.; Lough, A.; Ozin, G. A.; Bedard, R. L.; Broach, R. *J. Mater. Chem.* **1998**, *8*, 721. (b) Jiang, T.; Lough, A.; Ozin, G. A.; Bedard, R. L. *J. Mater. Chem.* **1998**, *8*, 733
(28) Sheldrick, W. S.; Wachhold, M. *Angew. Chem., Int. Ed. Engl.* **1997**, *36*, 206.

component to the hydrogen bonding[29] that removes electron density from the filled Cu−Cl σ^* orbitals could possibly account for the observation that the shortest Cu−Cl bond in **1** (Cu(2)−Cl(5) = 2.277(3)) corresponds to the chloride with the strongest hydrogen bond interactions, whereas the longest Cu−Cl bonds (Cu(1)−Cl(2) = 2.433(2) Å and Cu(1)−Cl(3) = 2.440(2) Å) in **1** correspond to the only chloride that sees effectively no hydrogen bond contacts.[6] (Note: in copper(I) chlorides there is no systematic difference between bridging and terminal Cu−Cl distances, both of which average 2.3 Å.) The methylammonium cations in **2** provide many more, albeit less defined, hydrogen bond contacts, complicating the evaluation of the influence of the hydrogen bonding.

Conclusions

The templated cuprous halides provide a useful system within which to explore the principles of crystal engineering and framework design. The relative influence of the charge density of both the inorganic building blocks and the template are shown to influence the extent and nature of network formation. The charge density of the inorganic species can be tuned stoichiometrically between the limits of the low charge density network, CuCl, to the high charge density molecular anion, $[CuCl_4]^{3-}$ as well as by the extent of network condensation within any given composition. High charge density templates within low charge density matrixes will favor the formation of higher dimensional network structures. Applying these principles to network constructions at the $[A]CuCl_2$ stoichiometry (A = monovalent cation), greater network condensation was achieved utilizing the higher charge density pyridinium and methylammonium templates than was previously achieved with the tetraethyl-, tetrapropyl-, and tetrabutylammonium or the dipositive methyl viologen or ethylenediammonium templates. These new network chains are constructed from trimeric, **1**, and tetrameric, **2**, secondary building units, respectively, which are analogous to a variety of group 13 chalcogenide materials. Furthermore, with utilization of these higher charge density templates in the relatively low charge density metal halide network, a micelle-like structural segregation between the templates and the metal halides was observed. This is most pronounced in the formation of the composite cation in **2**; but also in **1**, the association of the two pyridinium cations in the channel structure is evidence of similar species segregation. The charge density based network design principles described and demonstrated here for the $[MX_2]^-$ stoichiometry of the cuprous halides can be generally applied to the design of numerous open-framework materials.

Acknowledgment. This work was supported by the National Science Foundation (DMR-9501370 and DMR-0072828) and instrumentation grant (CHE-9509532). J. D. Martin is a Cottrell Scholar of the Research Corporation.

CM0006648

(29) Thompson, W. H.; Hynes, J. T. *J. Am. Chem. Soc.* **2000**, *122*, 6278.